SERS-active metal-dielectric nanostructures integrated in microfluidic devices for label-free quantitative detection of miRNA

Faraday Discussions

Accepted Manuscript

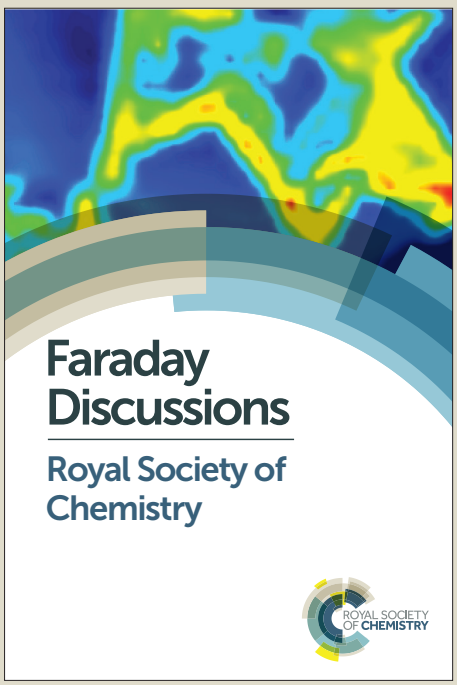

This article can be cited before page numbers have been issued, to do this please use: C. Novara, A. Chiadò, N. Paccotti, S. Catuogno, C. L. Esposito, G. Condorelli, V. de Franciscis, F. Geobaldo, P. Rivolo and F. Giorgis, *Faraday Discuss.*, 2017, DOI: 10.1039/C7FD00140A.

ROYAL SOCIETY OF CHEMISTRY

www.rsc.org/faraday_d

SERS-active metal-dielectric nanostructures integrated in microfluidic devices for label-free quantitative detection of miRNA

View Article Online
DOI: 10.1039/C7FD00140A

Chiara Novara[a,‡], Alessandro Chiadò[a,‡], Niccolò Paccotti[a], Silvia Catuogno[b], Carla Lucia Esposito[b], Gerolama Condorelli[b,c], Vittorio De Franciscis[b], Francesco Geobaldo[a], Paola Rivolo[a] and Fabrizio Giorgis[a,*]

[a]*Department of Applied Science and Technology, Politecnico di Torino, C.so Duca degli Abruzzi 24 10129,Turin, Italy*

[b]*Institute of Endocrinology and Experimental Oncology of Italian National Research Council, Via De Amicis 95 80145, Naples, Italy*

[c]*Department of Molecular Medicine and Medical Biotechnology, "Federico II" University of Naples, Naples, Italy*

*Corresponding author

‡ These authors contributed equally to this work.

In this work, SERS-based microfluidic PDMS chips integrating silver-coated porous silicon membranes were used for the detection and quantitation of microRNAs (miRNAs), which consist of short regulatory non-coding RNA sequences typically over- or under-expressed in connection with several diseases such as oncogenesis. In detail, the metal-dielectric nanostructures, which provide noticeable Raman enhancements, were functionalized according to a biological protocol, adapted and optimized from an enzyme-linked immunosorbent assay (ELISA), for the detection of miR-222. Two set of experiments, based on different approaches were designed and performed, yielding a critical comparison. In the first one, the labelled target miRNA is revealed through the hybridization to a complementary thiolated DNA probe, immobilized on the silver nanoparticles. In the second one, the probe is halved in shorter strands (half1 and half2) that interact with the complementary miRNA in two steps of hybridization. Such approach, taking advantage of the Raman labelling of half2, provides a label-free analysis of the target. After a suitable optimisation of the procedures, two calibration curves allowing quantitative measurements were obtained and compared on the basis of the SERS maps acquired on the samples loaded with several miRNA concentrations. The selectivity of the two-step assay was confirmed by the detection of target miR-222 mixed with different synthetic oligos, simulating the hybridization interference coming from similar sequences in real biological samples. Finally, that protocol was applied to the analysis of miR-222 in cellular extracts by using an optofluidic multichamber biosensor, confirming the potentialities of SERS-based microfluidics for early-cancer diagnosis.

Introduction

Solid Surface Enhanced Raman Scattering (SERS) platforms are characterized by a stable arrangement of metal nanoparticles (NPs), which can be assembled on carefully selected semiconducting/dielectric substrates with peculiar functional properties. Therefore, compared to colloidal systems, the solid ones ensure an improved stability concerning the electromagnetic enhancement of the Raman scattering generated by the interaction of molecules with the metallic NPs, which depends on the intense electromagnetic fields induced by the resonant excitation of Localized Surface Plasmons of the metal nanostructures. On the other hand, the substrate can act as a source of additional Raman chemical enhancement through charge transfer processes or as a high specific surface area, besides allowing an easy microfluidic integration for the development of point of care devices.[1–3]

In the last years, a growing number of applications of the SERS analysis related to biosensing was developed, thanks to its extraordinary sensitivity towards different targets in a large range of concentrations.[4,5] This technique has been applied for the determination of pathogens such as bacteria[4,6,7] or viruses[8], and of various biomarkers, such as metastatic cell's ligand peptides[9], and relevant blood biomarkers such as microRNAs[10].

Nowadays, miRNAs represent one of the most studied class of biomarkers[11] that consist in a large family of small non-coding RNAs composed by 20-22 nucleotides[12]. They control gene expression through post-transcriptional regulation via either translational repression or mRNA turnover, and so they are involved in a great number of biological processes including differentiation, development, cell proliferation and apoptosis.[13–15] As a consequence, their aberrant expression has been associated with many diseases, genetic disorders, and oncogenesis.[16] miRNAs are featured by a small size, a certain sequence similarity and a high variability in their expression levels.[16] Furthermore, a single gene can be regulated by different miRNAs, but, at the same time, a single miRNA can regulate different target genes.[17] Currently, most of the miRNA detection methods involves the use of fluorescent reporters, which require complex instrumentation and expensive chemicals, as is the case of the microarray technology and quantitative Polymerase Chain Reaction (qPCR), the most widely applied techniques for miRNA profiling.[11] For all of these reasons, new specific and sensitive analysis, characterized by a large dynamic range and a label-free approach, are still required for the detection of miRNAs.

Owing to its high sensitivity and specificity, reliable quantification, and multiplexing ability in the detection of oligonucleotides[18–20], SERS can be regarded as a possible solution for miRNA profiling of biological samples[21]. However, most of the literature related to the application of SERS to the analysis of miRNAs was obtained by the investigation of colloidal systems, of simply physisorbed molecules, or through very complex techniques based on non-enzymatic strand-displacements and on conformational changes of the probes.[22–25] Recently, highly sensitive substrates, that in optimized conditions are able to reach low Limit of Detection (LOD)[26], have been reported and integrated in a microfluidic chip, specifically designed to carry out multiplexing analysis[2]. They consist of a silver-decorated porous silicon (pSi) membrane supported on an elastomeric polydimethylsiloxane (PDMS) matrix. Thanks to the presence of a homogeneous distribution of silver NPs obtained by *in situ* synthesis, they generate an intense Raman enhancement, maintaining a good uniformity of the SERS signal intensity[26]. They can be synthesized on large areas, avoiding expensive and time-consuming top-down nanolithography techniques such as electron-beam lithography (EBL) and/or focus ion beam lithography (FIB), devoted to the fabrication of periodically ordered plasmonic nanostructures. Moreover, they show a great physico-chemical stability that is reflected into the retention of the plasmonic response even after the incubation in those buffers typically used for bioassays[26]. Therefore, they are good candidates for the development of biosensing devices for challenging biological analytes, such as miRNAs.

In this paper, it is reported the application of these metal-dielectric nanostructures to the detection of miRNA. In particular, two different approaches were designed and compared. The first one consisted in the immobilization of a thiol-capped DNA probe on the silver NPs to detect the complementary labelled target miRNA. This protocol, previously developed as an enzyme-linked immunosorbent assay (ELISA) for metal-dielectric substrates, was further optimized for the SERS analysis. On the other side, a second approach characterized by a label-free detection of miRNAs, in which the probe is halved in two strands (half1 and half2), was also investigated and optimized. In this case, the first strand of the original probe (half1) is immobilized on the surface and captures the specific miRNA from the sample, whereas the SERS detection is assisted by the following hybridization of the leftover of the probe, the second strand (half2), which is labelled with a Raman dye. For the initial tests, the miR-222 was selected as model miRNA because of its involvement in numerous neoplastic diseases, such as lung, brain, liver, renal, prostatic and pancreatic cancer.[27–29] The two protocols were carefully optimized, with a particular attention to the optimal surface probe density, which was identified with a series of experiments conducted with different concentrations of probes incubated in buffers at different ionic strengths, followed by the hybridization and detection of a labelled complementary miRNA. Afterwards, two different Raman labels, Cyanine 3 (Cy3) and Cyanine 5 (Cy5) were tested, allowing the fruitful comparison of the calibration curves obtained by SERS mapping of the samples incubated with various concentration of target miRNA and treated with the different approaches. Then, the two-step hybridization assay, which showed a low LOD in a label-free configuration, was used to specifically detect the miR-222 mixed with other synthetic miRNAs, simulating the hybridization interference coming from the incubation of the system with real samples. The main results were confirmed by ELISA. Finally, the target miRNA was successfully detected into cellular extracts by using the optofluidic chip.

Experimental

Materials and chemicals. DL-dithiothreitol (98.0% DTT), acetic acid (99.0%), Bovine Serum Albumin (BSA, IgG free), polyethylene glycol sorbitan monolaurate (tween), sodium acetate (99.0%), sodium chloride (99.5%), tris(hydroxymethyl)aminomethane (TRIS), ethanol (> 99.8%), ethylenediaminetetraacetic acid (EDTA, 99.4%), saline sodium citrate (SSC, sterile stock 20x, 300 mM trisodium citrate, 3 M NaCl), sodium dodecyl sulfate solution (BioUltra, 10%, SDS), 3,3',5,5'-tetramethylbenzidine (TMB), heat-inactivated fetal bovine serum, L-glutamine and penicillin-streptomycin were from Sigma Aldrich, Milan, IT. All the DNA and RNA oligos were from Sigma Aldrich, Milan, IT, and from Integrated DNA technologies, Leuven, BE. HF was from Carlo Erba, Milan, IT. PDMS pre-polymer and curing agent (Sylgard 184) were from Dow Corning. Horseradish Peroxidase conjugated Streptavidin (Str-HRP) was purchased from Jackson ImmunoResearch Europe Ltd. (Suffolk, UK). The RPMI 1640, the mirVana miRNA isolation kit were from Life Technologies, Milan, IT. The Opti-MEM and Lipofectamine 2000 were from Invitrogen (Life Technologies, Milan, IT). Illustra MicroSpin G-25 columns were from GE Healthcare (Fisher Scientific, Illkirk, FR). Water used during each step was Milli-Q™ dispensed from a DirectQ-3UV (Merck-Millipore, Milan, IT) and sterilized. Human NSCLCC H460 were from the American Type Culture Collection (Manassas, VA, USA). The miR-222 precursor was from Ambion (Life Technologies, Milan, IT). The TRiFast total RNA extraction kit was from Euroclone, Milan, IT. The miScript Reverse Transcription kit, the miScript-SYBR Green PCR Kit and the specific miScript Primer Assay kit were from Qiagen, Milan, Italy).

Fabrication of SERS substrates. The PDMS-supported pSi (PSD) samples integrated in the microfluidic chambers were fabricated as detailed elsewhere[2,26]. Concerning the SERS-active metal-dielectric nanostructures, pSi was prepared by electrochemical etching (125 mA/cm^2, 30 s) of highly boron-doped silicon wafers (34-40 mΩ-cm resistivity), in HF solution (20:20:60 HF/H_2O/CH_3CH_2OH) at room temperature. The pSi was then detached from the original Si substrate by anodization (4 mA/cm^2, 95 s) in a low concentrated ethanolic HF electrolyte (4%). The produced membranes were readily transferred by stamp and peel-off from the initial Si substrate by using a partially cross-linked PDMS slice obtained by casting and curing (80 °C, 10 min) a 10:1 w/w mixture of oligomer and curing agent. The silver NPs were synthesized in situ by dipping the pSi/PDMS membranes in an aqueous 10^{-2} M $AgNO_3$ solution supplemented with ethanol 2.5% v/v and HF 0.0006% v/v for 2 minutes at 50 °C. Afterwards, the integrated PSD membranes were pretreated by one-hour incubation in 1% BSA in 50 mM sodium acetate buffer pH 4.0, in order to reduce the nonspecific binding. Finally, they were washed in TE buffer (10 mM Tris, 1 mM EDTA, pH 7.5) to remove the protein excess.

One-step and two-step hybridization bioassay on the solid SERS substrates. An ELISA-like protocol developed in 96-well plates, and optimized for metal-dielectric substrates[26], was used and further modified to detect the miR-222 (5'-AGCUACAUCUGGCUACUGGGU-3') by SERS analysis. In particular, two different procedures, based on different probes were used. In the first one (Fig.1a), the target miRNA is detected through a one-step hybridization to a complementary 22-nucleotide-long thiolated DNA probe (probe222, 5'-C6SH-ACCCAGTAGCCAGATGTAGCT-3') immobilized on the silver NPs. Instead, in the second one (Fig.1b), the probe is halved in two shorter sequences, half1 (5'-C6SH-ACCCAGTAGC-3') and half2-CyX (5'-CAGATGTAGCT-Cy3/Cy5-3'). The former is immobilized on the surface and catches the specific miRNA from the sample, whereas half2, which is modified with a Raman label, allows the detection in two hybridization steps. Both the probes were DTT-reduced, desalted (Illustra MicroSpin G-25 columns) and quantified before the immobilization on the PSD samples by overnight incubation in TE-NaCl (TE, 1M NaCl, pH 7.5). The detailed reduction and desalting protocol can be found elsewhere[26]. In order to find the optimal conditions for the analysis, different concentrations of probes (1-50 µM) and/or of NaCl (0-2 M) in TE buffer were investigated. Negative controls were as well incubated overnight in TE-NaCl without the probe (no-probe control). After overnight incubation, the samples were washed thrice in TE-t (TE, 0.05% tween, pH 7.5) to remove the nonspecific binding and blocked with 1% BSA in TE. For what concerns the miRNA hybridization step, different conditions were employed for the one-step and two-step hybridization procedures. In the one-step bioassay, after the BSA-blocking step the samples were incubated for 1 hour with 25 µL of miRNA at different concentration in SSC 4x-SDS (0.01% SDS, pH 7.5), and then washed trice with SSC 1x-SDS (0.01% SDS, pH 7.5). The same immobilization protocol was used for the two-step bioassay, unless that, after the BSA-blocking step, the miRNA was incubated in SSC 5x-SDS (0.01% SDS, pH 7.5) and then the samples were washed in SSC 4x-t (0.05% tween, pH 7.5). Afterwards, the substrates were incubated with 25 µL of 1 µM half2 in SSC 5x-BSA-t (0.05% tween, 1% BSA, pH 7.5) for 1 hour and washed three times with SSC 4x-BSA-t (0.05% tween, 1% BSA, pH 7.5). A test with various mixtures of miR-222 and miR-16 (5'-UAGCAGCACGUAAAUAUUGGCG-3'), at different molar concentrations, was used to confirm the specificity of the two-step bioassay.

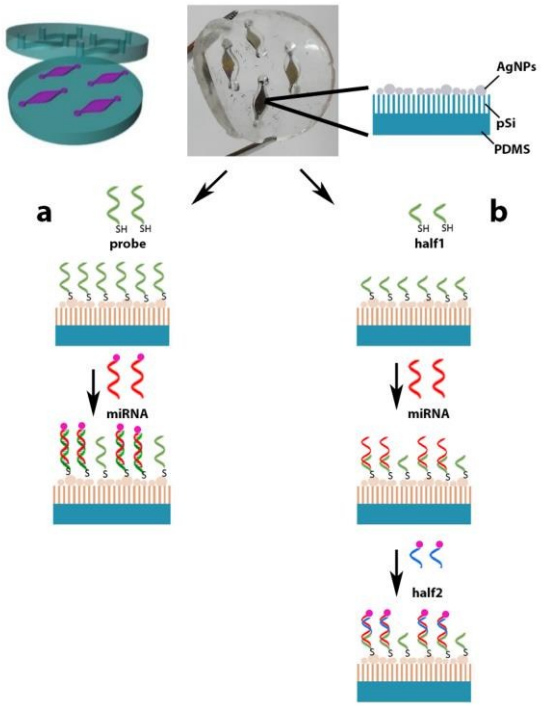

Fig. 1. Microfluidic chip integrating pSi membranes decorated by Ag NPs and detection schemes of miRNA by (a) one-step hybridization assay (b) two-step hybridization assay.

ELISA-like protocol on the solid SERS substrates. The ELISA-like bioassay was used as a reference technique for the Raman results. The same protocol reported above was applied on the SERS substrates. In this assay a 5'-biotinylated miR-222 (5'-biotin-AGCUACAUCUGGCUACUGGGU-3') and a 3'-biotinylated half2 (5'-CAGATGTAGCT-biotin-3') were employed for the one-step and two-step hybridization bioassays, respectively, instead of the cyanine labelled miRNA/half2. After the last incubation and washing steps, the samples were incubated with 25 µL of 0.5 µg/mL Str-HRP in SSC 4x-SDS for the one-step protocol, or in SSC 4x-BSA-t for the two-step protocol. Then, the samples were washed trice with the same buffer used for the incubation and developed. Briefly, the TMB substrate solution was added onto the samples to initiate the colorimetric reaction, which was stopped after 2 minutes adding H_2SO_4 (0.5 M), with a 1:1 TMB:H_2SO_4 ratio. The Optical Density (OD) of the solution was immediately measured at 450 nm and at 630 nm by means of a 2100-C microplate reader (Ivymen Optic System). The amount of probe immobilized on the surface was indirectly quantified with an in-liquid titration curve of Str-HRP serial diluted in Milli-Q™, whose OD was measured after the reaction with TMB. The OD recorded for the different samples was normalized and transformed in surface density (molecules/cm^2)

DOI: 10.1039/C7FD00140A

by comparison with the in-liquid titration curve and using a factor of 50, as Str/probe surface ratio, as previously reported.[30,31] Several replicates for each experimental condition were analysed and the error bars reported on the histogram diagrams concerning with colorimetric ELISA-like measurements represent the standard deviations (SD).

SERS analyses. The SERS substrates, functionalized according to the one/two-step protocols, were used for the Raman detection of the miR-222. The samples were dried under a nitrogen stream and analysed with a Renishaw InVia Reflex micro-Raman spectrometer (Renishaw plc, Wotton-under-Edge, UK) with a 514.5 nm laser excitation in backscattering light collection under a long working distance 100x objective. In particular, the samples were analysed after the BSA blocking step (immobilized probe), after the hybridization of the miRNA and at the end of the second hybridization for those samples incubated with the half2. All the spectra were acquired by mapping the surface of the samples over a 50 µm X 40 µm area, with a 5 µm step. All the samples were analysed using a low laser power density (0.025 mW with a defocused exciting optical spot) in order to avoid the degradation of the biomolecules. The data obtained from the SERS measurements were processed through the hyperSpec package[32] in R (R 2017, R Foundation for Statistical Computing, Vienna, Austria. https://www.R-project.org/.)[33]. In addition, the spectra used for the calibration of the SERS intensity vs. miRNA concentration were analysed with the curve fit routine provided by the Wire 3.4 Renishaw software. Finally, the LOD was calculated using the mean value of the blank samples plus three times their SD, considering the linear range of the calibration curves (Raman signal intensity vs. miRNA concentration) for each protocol.

Detection of miR-222 in cell extracts. The RNA cell extract were obtained from Human NSCLCC H460 and miR-222-transfected H460 cells, grown in RPMI 1640 supplemented with 10% heat-inactivated fetal bovine serum, 2 mM L-glutamine and 100 U/ml penicillin-streptomycin. All transfections were performed using the serum-free Opti-MEM and Lipofectamine 2000 reagent according to the manufacturer's protocol. H460 cells were transfected with 100 nM of the miR-222 precursor for 48 hours. The total RNA samples were extracted with TRiFast kit, whereas small RNA-enriched samples were prepared by using mirVana miRNA isolation kit. Then, in order to detect the miR-222 in the cell extracts, the two-step hybridization bioassay was used. After the immobilization of half1, the samples were incubated with the cell extracts diluted 1:2 in SSC 10x to a final concentration of 5x. The labelled half2 (-CyX or -biotin in case of SERS or ELISA-like assay, respectively) was then incubated, by following the same conditions described above. The miR-222 expression levels in all the tested RNA cell extracts was obtained by Reverse Transcription quantitative Polymerase Chain Reaction (RTqPCR). For Real-time PCR, 500 ng of RNA was reverse transcribed with miScript Reverse Transcription kit, then amplified by using the miScript-SYBR Green PCR Kit and specific miScript Primer Assay. U6 RNA was used as a housekeeping control gene. miRNA expression was measured using Ct (threshold cycle) and the ΔΔCt method for relative quantization of gene expression.

Results and discussion

Recently, an ELISA-like assay for the detection of miRNAs on metal-dielectric substrates has been developed.[26] That study was devoted to the optimization of a biofunctionalization protocol based on a single probe-miRNA hybridization approach, which can be transferred to other analytical techniques that exploit metal-dielectric nanostructures, including SERS spectroscopy. Particular attention was also paid to the integrity of the substrates after the several incubation steps in the buffers needed for the bioassay. Among the studied metal-dielectric nanostructures, the PDMS-supported pSi (PSD) samples were tested as well, showing the highest SERS enhancement and the best uniformity, even at the end of the whole assay. Here, this one-step hybridization protocol has been applied to the PSD samples, in order to perform the detection of miRNAs by SERS analysis. At the same time, a new procedure based on two steps of hybridization has been developed to allow the direct label-free detection in cellular extracts.

Fig. 1 compares the schemes of the two approaches. Both are performed on a multichamber microfluidic chip integrating metal-dielectric nanostructures, where the analysis can be conducted on reduced sample volumes under controlled analyte injection conditions mitigating potential contamination problems. The one-step protocol (Fig. 1a) theoretically allows the label-free analysis of miRNAs based on their vibrational fingerprints, but it is practically affected by the typical issues of SERS detection of oligonucleotides hybridization, such as the very similar SERS signals of probes and targets[8]. Conversely, the two-step protocol enables the recognition of specific miRNAs, thanks to the immobilization of half1 on the NPs, followed by the detection mediated by half2, which can be conjugated to a Raman label, after the second hybridization step. Such analytical procedure takes advantage of the intense and clearly distinguishable vibrational pattern of the label, without any modification of the target. Nevertheless, because of the halved number of nucleotides involved in each hybridization of the two-step assay, the probe/miRNA interaction is weaker. In order to allow the direct comparison between the results obtained from the two procedures, a labelled miRNA-CyX (X=3 or 5) is therefore employed for the one-step protocol.

Optimization of the one-step and two-step hybridization assays for the detection of miRNA by SERS analysis. From the biochemical point of view, the functionalization of the PSD substrates according to the one- and two-step approaches requires an accurate tuning of the immobilization and incubation conditions, which are expected to be different due to the varied length of the probe and to the peculiar probe-miRNA interactions. The step-by-step SERS analysis during the protocol provides direct insight on the surface phenomena and was exploited for its optimization.

At first, the minimization of the nonspecific binding of the target, related to its random interaction with the surface, was investigated by measuring the Raman spectra of the SERS substrates pretreated with BSA and incubated with a Cy5/Cy3-labelled

miRNA/half2 dissolved in the buffers used at the hybridization step of the different protocols, in the absence of the probe immobilized on the silver NPs. After 1 hour of incubation, the samples were washed in the same buffer and analysed. Different compositions were applied for the one-step and two-step assays, because the room temperature hybridization of the miRNA requires a higher ionic strength for the washings of the two-step hybridization approach. As mentioned above, in this case only ten base pairs are formed between the half1/half2 and the miRNA, lowering the melting temperature of the complex.

The main results of this test are shown in Figs. 2a (miRNA-CyX) and 2b (half2-CyX). The spectra recorded on the samples without any surface blocking pretreatment are reported on the top of each graph as a reference. Expectedly, all these spectra are dominated by the vibrational fingerprints of the cyanine dyes, as shown by the similarity between the modes observed for miRNA-CyX and half2-CyX modified with the same Raman label. In particular, the most intense bands are attributed to the C=N stretching of the ring atoms, to the CH_3 deformation of the ring substituents and to the methine chain vibrations typical of indocarbocyanines.[34] The modes are located around 1589 cm^{-1}, 1463 cm^{-1}, and 1352 cm^{-1} for Cy5[9], while a shift toward 1388 cm^{-1} is observed for the last band in case of Cy3, which presents a shorter bridging chain[35]. The analysis of the bare substrates clearly points out that in the absence of a surface passivation a certain degree of nonspecific binding exists. On the other hand, the use of high surfactant concentrations in the immobilization/hybridization steps, which can minimize the non-specific binding, is detrimental for the specific hybridization as well and should be avoided. Indeed, the Raman signal of the label significantly decreases, regardless of the buffer composition and for both the tested protocols, if the sample is pretreated with BSA (Fig. 2, black spectra). At the same time, the addition of a surfactant (tween or SDS) in the washing buffers improves the nonspecific binding removal, as highlighted by the comparison of the spectra acquired for the miRNA-CyX incubated in SSC 1x or SSC 4x with those recorded in the same buffers supplemented with 0.01% SDS. The same effect is observed with the half2-Cy5 incubated in SSC 4x or in SSC 4x-SDS, despite the higher non-specific signal probably due to the smaller size of the shorter sequence. Instead, the typical features of half2-Cy3 can still be distinguished from the background spectrum, arising from the BSA pretreatment, even after the washings in SSC 4x-SDS. The persistence of Cy3 vibrational signal is not related to a higher surface affinity, but is probably the consequence of the resonant analysis of Cy3 by means of the 514.5 nm laser excitation. Under these conditions, the SERS spectrum of the dye is enhanced compared to the electronic off-resonance condition of the Cy5 label. For the same reason, a lower LOD can be reached by the exploitation of Cy3 electronic resonance. Then, in order to obviate the higher non-specific signal, 1% BSA was added to the washing buffer after the half2 incubation, and SDS was replaced with tween 0.05%. By means of this ploy, the intensity of the SERS signal of the label was effectively reduced, as reported on the bottom of Fig. 2b. These results highlight the need for a surface pretreatment of the PSD samples and the positive impact of the surfactants in the washing buffers.

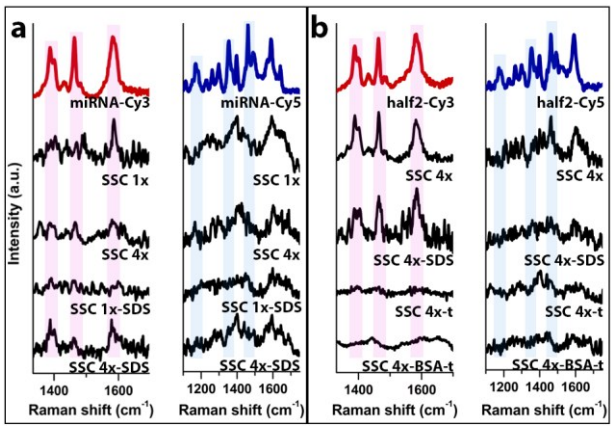

Fig. 2 a) Evaluation of the non-specific SERS signal given by the labelled miRNA (Cy3 on the left, Cy5 on the right) incubated in the buffers used for the one-step hybridization assay (SSC 1x, SSC 4x, SSC 1x 0.01% SDS, SSC 4x 0.01% SDS) followed by washings in the same buffers; b) Evaluation of the non-specific signal given by the labelled half2 (Cy3 on the left, Cy5 on the right) incubated in the buffers used for the two-step hybridization assay (SSC 4x, SSC 4x 0.01% SDS, SSC 4x 0.05% tween, SSC 4x 0.05% tween 1% BSA) followed by washings in the same buffers. On top of each series, the reference spectra of the spotted labelled target are reported. The main vibrational bands of the labels are highlighted.

Once the buffer composition was adjusted to minimize the nonspecific signal, the optimal probe concentration and the ionic strength of the immobilization buffer were investigated, in order to maximize the miRNA hybridization, and consequently the related SERS spectral intensity. Actually, the probe density is a fundamental parameter, which should be as high as possible to maximize the detected hybridization signal, but at the same time, avoiding steric hindrance due to tightly packed probe molecules.[36] In contrast to other techniques, the direct evaluation of the amount of probe immobilized on the surface given by SERS analysis, allows an incomparable opportunity for the optimization of this parameter.

At the beginning, the probes (probe222 and half1) were DTT-reduced and incubated in a concentration range from 1 to 50 µM (TE, 1M NaCl). Fig. 3a shows the related SERS spectra of the probe222. The typical Raman features of the oligoprobe, mainly assignable to the vibrational modes of the nucleobases, appear at 1 µM concentration emerging from the BSA background signal. In particular, the ring breathing modes (adenine at 730 cm^{-1}, cytosine and thymine at 790 cm^{-1})[37], the adenine ring stretching (1325 cm^{-1})[37] and the typical guanine bands at 1480 cm^{-1}(C-N stretching/N-H bending) and 1580 cm^{-1},[38] together with an adenine related-shoulder at 1577 cm^{-1} (NH_2 scissoring)[39] can be identified. A distinct band at 1636-1640 cm^{-1} represents the carbonyl stretching of the pyrimidine bases[40], while weaker deoxyribose and PO^-_2 stretching modes are detected at 1030 and 1096 cm^{-1}.[39] Their intensity increases along with the concentration of incubated probe. At the same time, the initial background characterized by the Raman peaks of BSA at 1660 cm^{-1} (amide I), 1453 cm^{-1} (protein side chain deformations), 1001 cm^{-1}, 1203 cm^{-1}, 1370 $cm^{-1}$and 1614 cm^{-1} (aromatic amino acids) is reduced.[41] These observations are in agreement with the occurred immobilization of the probe on the surface, which displaces the protein. Moreover, a certain surface saturation is observed for concentrations higher than 25 µM. This saturation is evident in Fig. 3b, in which the integrated area of the isolated pyrimidine ring breathing mode at 790 cm^{-1} is plotted vs. the concentration of the probe.

The functionalized samples were successively incubated with 1 µM miR-222-Cy5, and analysed by SERS. The whole vibrational pattern of the dye is clearly detectable in the acquired spectra (Fig. 3c), even for the lowest probe concentration. The highest hybridization signal is obtained if the probe is incubated with a 25 µM solution, while the Raman intensity weakly decreases upon further increase of the probe concentration, as pointed out by the trend of the integrated area of the Cy5 band located at 552 cm^{-1} (C-C(CH_3)-C moiety of the ring[34], Fig. 3d). Therefore, the optimal probe222 density is attained at concentration of 25 µM.

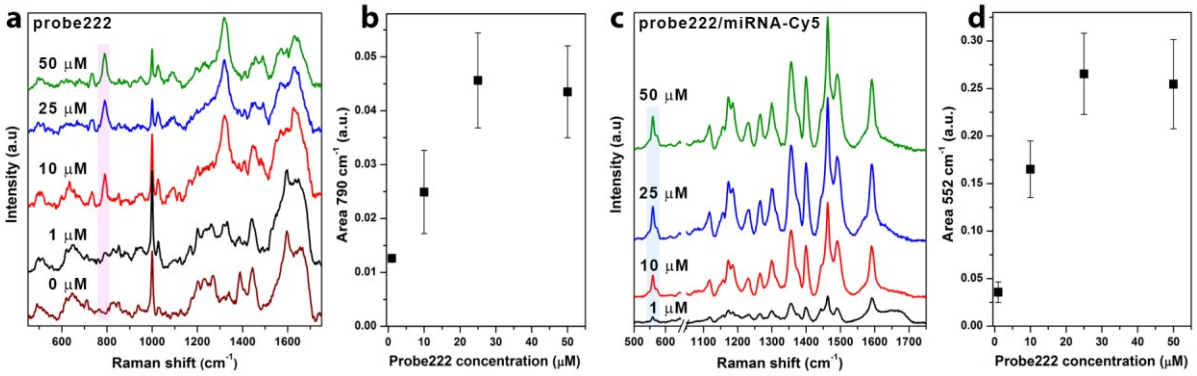

Fig. 3 Evaluation of the optimal concentration of probe222: a) SERS spectra of the substrates incubated with different concentration of probe222; the spectrum of a substrate pretreated with BSA is shown as a reference (brown curve) b) integrated areas of the 790 cm^{-1} Raman peak of the probe vs. its immobilization concentration; c) SERS spectra of the same samples after the incubation with 1 µM miR-222-Cy5; d) integrated area of the miRNA-Cy5 Raman peak at 552 cm^{-1} vs. the probe222 immobilization concentration. The error bars correspond to the SD.

Concerning the two-step bioassay, the evaluation of the half1 concentration necessary to obtain an optimal probe density was performed in a similar way. In order to allow a better comparison between the two protocols, the same concentrations of probe and of labelled miR-222 were applied. Fig. 4a reports the spectra acquired after the incubation of half1 at different concentrations. Although it only consists of 10 nucleotides, its vibrational pattern is analogous to the one detected for the 22-nucleotides long probe222. This result proves that the main contribution to the SERS spectra of the probes is provided by the bases that are closer to the silver surface, as previously suggested in the literature[42]. Similarly to the previous experiment, the spectra reveal that a saturation regime is attained around 25 µM, for which the integrated area of the 790 cm^{-1} band reaches its maximum Fig. 4b). Then, the samples were incubated with 1 µM miR-222-Cy5 in order to directly compare the hybridization signal of the one-step and two-step procedures (Fig. 4c). The highest SERS intensity is however detected when the probe is incubated at a concentration of 10 µM, while for the lower concentrations the hybridization signal decreases and, for the higher ones, approaches a saturation plateau, as indicated by the integrated area of the 552 cm^{-1} of the Cy5 (Fig. 4d). Therefore, such a concentration is selected for the immobilization of half1 for the two-step bioassay.

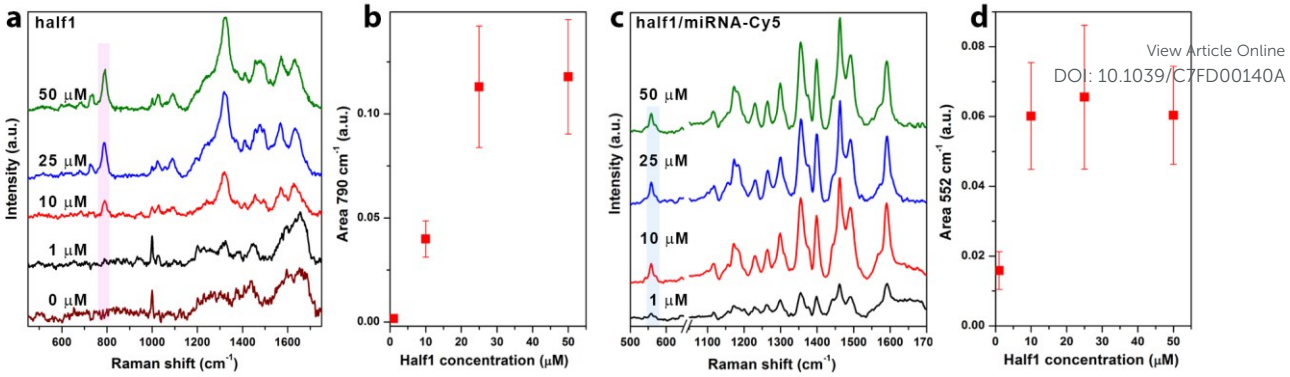

Fig. 4 Evaluation of the optimal concentration of half1: a) SERS spectra of the substrates incubated with different concentration of half1; the spectrum of the substrate pretreated with BSA is shown as a reference (brown curve) b) integrated areas of the 790 cm^{-1} Raman peak of the half1 vs. its immobilization concentration; c) SERS spectra of the samples after the incubation with 1 μM miR-222-Cy5; d) integrated area of the miRNA-Cy5 Raman peak at 552cm^{-1} vs. the half1 immobilization concentration. The error bars correspond to the SD.

As extensively reported in the literature[36,43], in order to obtain an optimal packing of the probes on the surface by self-assembly, a certain amount of salt is required in the immobilization buffer to shield the negative charges carried by the phosphate groups of the probe backbone. However, only an indirect evaluation is usually obtained or an awkward approach is required by means of standard techniques, such as ELISA, Surface Plasmon Resonance or X-ray photoelectron spectroscopy[36,43,44]. Instead, the amount of immobilized probe can be directly assessed by SERS analysis. Therefore, the evaluation of the optimal ionic strength was carried out for the one-step and two-step protocols, as a check of the value previously inferred by the ELISA-like tests optimized on the same metal-dielectric substrates[26]. The probe222 or the half1 were incubated on the substrates in TE supplemented with increasing concentration of NaCl and analysed. Concerning the one-step approach, the results of the SERS analysis reported in Fig.5a highlight that few and weak Raman features of the probe222 start to characterize the acquired spectra from 50 mM of NaCl. The intensity of these peaks increased along with the NaCl concentration, without reaching a surface saturation, neither at the highest tested concentration of 2M NaCl. Then, the same samples were incubated with 1 μM miR-222-Cy5. Despite the monotonic increase of the amount of immobilized probe, the highest hybridization signal is reached at 1M NaCl (Fig. 5d), suggesting that the excessive probe packing significantly reduces the hybridization efficiency at higher salt concentrations. These results were confirmed by the integration of one of the main peaks of the probe and of the Cy5 label, as reported in Fig. 5c,f (black squares).

The same tests were repeated for the two-step hybridization assay. The spectra acquired after the incubation of the half1 (Fig. 5b), similarly to the other approach, confirmed that the amount of probe immobilized on the surface increased along with the ionic strength, without reaching a saturation regime. At the same time, the highest amount of labelled miRNA hybridized to the half1 was observed for 1M NaCl (Fig. 5e). These outcomes were confirmed by evaluating the area of the main peaks, as reported in Fig. 5c and f (red dots). It is worth to notice that a higher amount of half1 is immobilized on the surface at the same ionic strength, and that the immobilization of the half1 started at lower concentration of salt, if compared to the probe222, as highlighted by the data trends reported in Fig. 5c. Probably this effect is due to the size and in particular to the different length of the two strands: the longest probe222 requires more ions to solvate all the negative charges of the backbone, in comparison to the shortest half1. These results are in accordance with the outcomes reported above, and related to the optimal concentration of probe incubated on the samples (Fig 3 and 4). In fact, by fixing the ionic strength at 1M NaCl, a lower concentration (10 μM) is required to obtain the optimal amount of half1 immobilized on the surface, in comparison with the probe222 (25 μM). Finally, thanks to the SERS analysis it was possible to verify that the optimal probe density needed for the highest hybridization of the corresponding miRNA is obtained before the surface saturation is reached. Then, once the optimal amount is achieved, the hybridization of miRNA does not change anymore, probably because of effects concerning the stability of the densely packed grafted probes or of the DNA-RNA complexes at relatively high salt concentration.

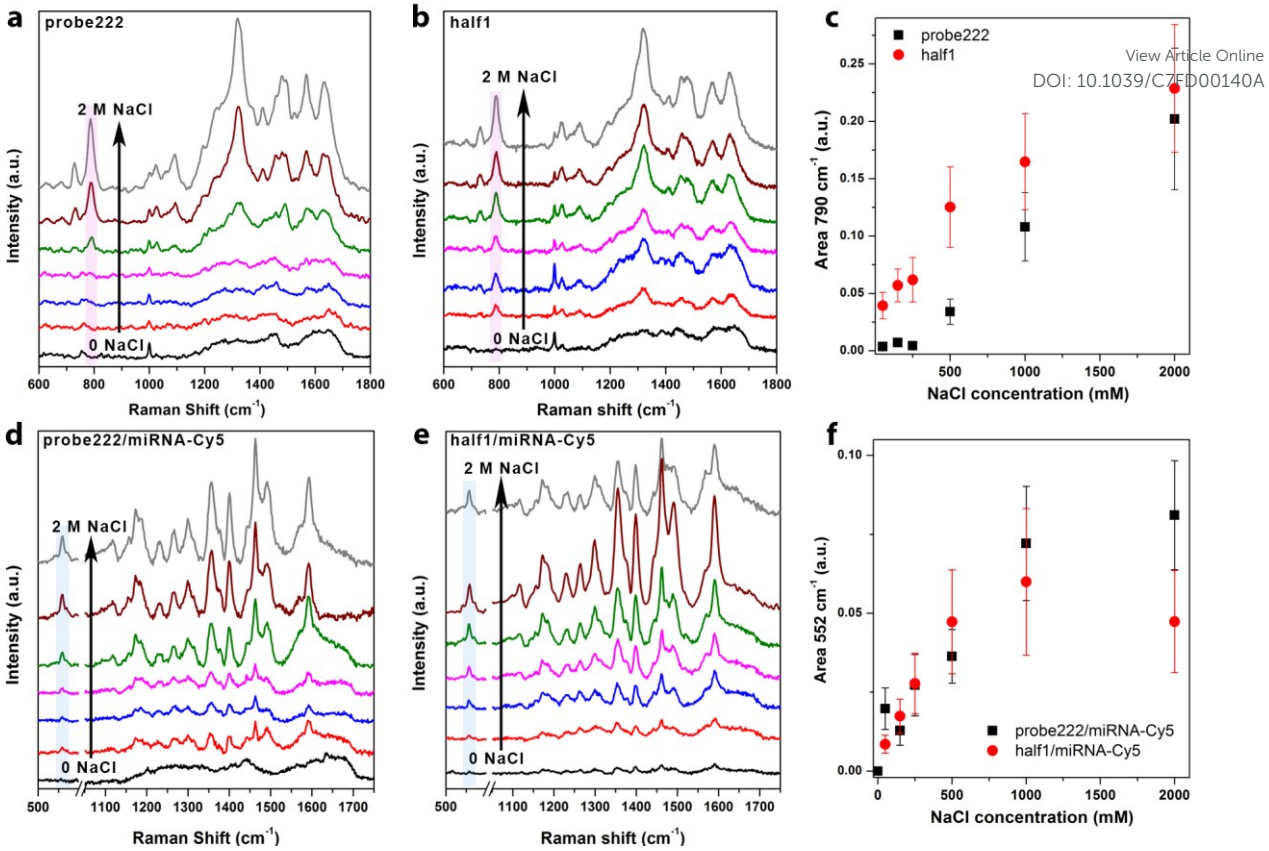

Fig. 5 Evaluation of the optimal ionic strength in the immobilization buffer: a) SERS spectra of the probe 222 (25 µM) incubated at different NaCl concentrations; b) SERS spectra of the half1 (10 µM) incubated with different NaCl concentrations; c) integrated areas of the 790 cm^{-1} Raman peak of the probe222 (black squares) and half1 (red dots) vs. the NaCl concentration; d) SERS spectra of the samples in Fig. 5a after the incubation with 1 µM miR-222-Cy5; e) SERS spectra of the samples in Fig. 5b after the incubation with 1 µM miR-222-Cy5; f) integrated area of the miRNA-Cy5 Raman peak at 552 cm^{-1} vs. the NaCl concentration for samples functionalized with the probe222 (black squares) and the half1 (red dots). The error bars correspond to the SD.

Specificity and sensitivity of the bioassays. After the optimization of the immobilization and hybridization conditions was completed, the one and two hybridization approaches were compared in terms of sensitivity, using both Cy5 and Cy3 as Raman labels. The PSD samples functionalized with the probe222 and half1 at the optimized concentrations were incubated with several concentrations of miRNA, from 0.1 nM to 1 µM. miR-222-CyX and an unlabelled miR-222 were employed at the first hybridization step for the first and second protocol, respectively. In the two-step approach, half2-CyX was finally incubated on the hybridized half1-miRNA substrates. Fig. 6a,b (Cy3) and d,e (Cy5) report the SERS spectra acquired on the described samples. The high concentrations are not shown because the saturation of the hybridization signal is reached over 500 nM. As expected, a stronger Raman intensity is observed for the Cy3 label, due to the excitation at its electronic resonance. Such result is reflected both in the Raman intensity, but also affects the minimum detectable concentration. In general, the spectra of Cy3-oligos are dominated by the vibrational fingerprints of the label, except for the lower miRNA concentrations, where the DNA probe pattern is superimposed to the target signal. The exam of such a background shows the presence of a less crowded region between 1450 and 1470 cm^{-1}, where one of the main peaks ascribable to the Cy3 can be conveniently identified even at the lower concentrations. The intense vibrational mode of Cy3 at 1462 cm^{-1} was therefore selected for the determination of the LOD. For what concerns Cy5-oligonucleotides, the spectrum of the probe starts to be overwhelming at medium-high concentrations of miRNA. However, the same spectral window can be exploited for the detection of Cy5 band at 1463 cm^{-1}, which is clearly detectable by eye until 25 nM. As a reference, the two-step assay was applied to a second set of PSD samples and treated by following the ELISA-like protocol. For completeness, the ELISA results are reported in the Electronic Supplementary Information (Fig. S1a).

In order to perform quantitative measurements, a calibration curve was prepared by the integration of the area of Cy5 and Cy3 bands at 1463 and 1462 cm^{-1}. The calculated areas are reported in log-log scale in Fig. 6c and 6f for Cy5 and Cy3, respectively. The data analysis reveals an interesting behaviour for the two-step hybridization procedure compared to the one-step approach, regardless of the used dye. Actually, the SERS spectra of the half1/miRNA/half2-CyX complex are characterized by a lower Raman signal intensity than their probe/miRNA-CyX counterparts in the high miRNA concentration regime. On the other side, in the

former, the spectral intensity referred to the miRNA hybridization is featured by a weaker decrease than in the latter, by lowering the nominal concentrations of miRNA.

View Article Online
DOI: 10.1039/C7FD00140A

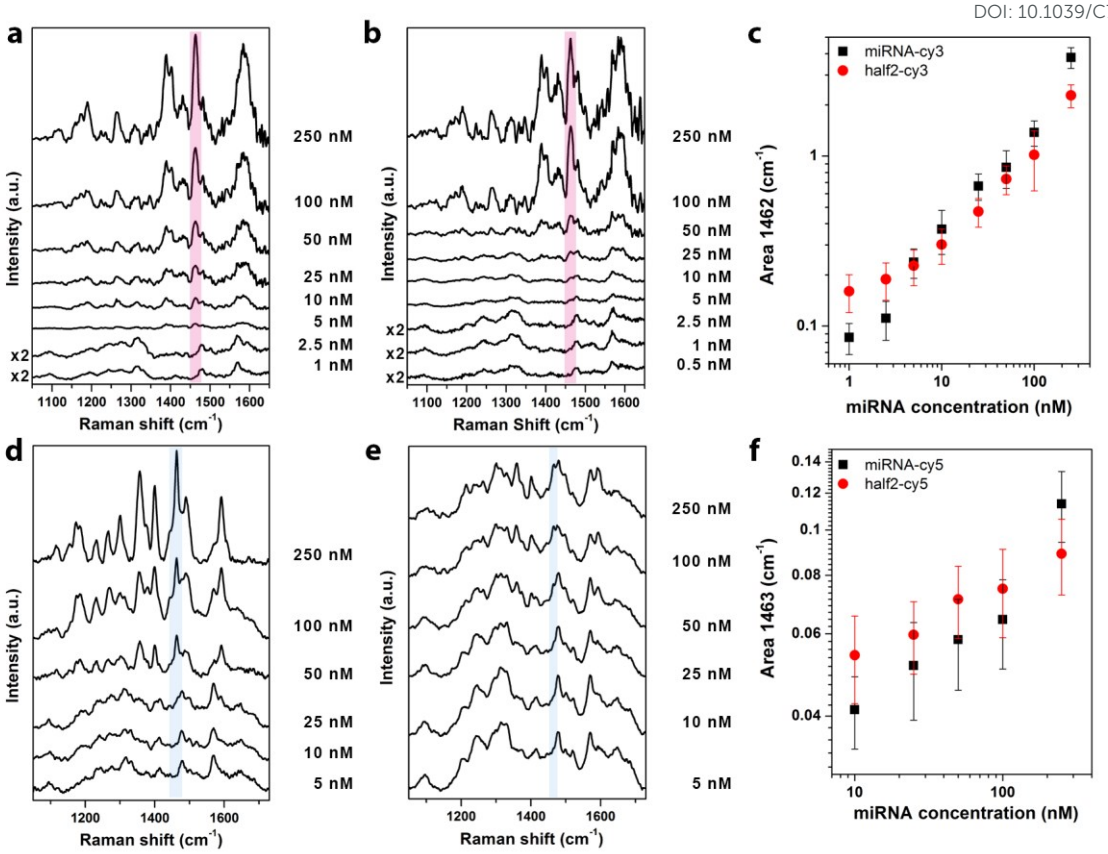

Fig. 6 a) SERS spectra of the functionalized samples incubated with different concentrations of miR-222-Cy3; b) SERS spectra of the functionalized samples incubated with different concentrations of miR-222 and subsequently with 1 µM half2-Cy3; c) Integrated area of Cy3 peak at 1462 cm^{-1} vs. miR-222 concentration, calculated for miR-222-Cy3 (black squares) and half2-Cy3 (red dots); d) SERS spectra of the functionalized samples incubated with different concentrations of miR-222-Cy5; e) SERS spectra of the functionalized samples incubated with different concentrations of miR-222 and subsequently with 1 µM half2-Cy5; f) Integrated area of Cy5 peak at 1463 cm^{-1} vs. miR-222 concentration, calculated for miR-222-Cy5 (black squares) and half2-Cy5 (red dots). The error bars correspond to the SD. The features of Cy3 at 1462 cm^{-1} and Cy5 at 1463 cm^{-1} are highlighted.

A portion of the investigated miRNA concentrations was employed for the calculation of the LOD involving the Cy3 dye. In particular, a linear regime was observed between 25 and 2.5 nM for miRNA-Cy3 and from 25 to 1 nM for the miR-222 detected by the half2-Cy3. The samples incubated with 0.5 nM miRNA-Cy3, and the control substrate incubated with half1 and half2-Cy3, without the miRNA hybridization step, were considered as the blanks in the two set of experiments. The different calibration curves provided similar detection limits of 0.55 and 1.51 nM for the one-step and two-step hybridization assays, respectively. Generally, a higher sensitivity could be expected for the one-step procedure than for the two-step hybridization one, due to the weaker interaction between half1 and the miRNA compared to the probe222-miRNA binding. Anyway, this disparity seems to be well compensated by the optimization of the hybridization conditions, such as the higher salt concentrations in the buffer, which improves the effectiveness of the interaction. These results ensure that the two-step procedure does not worsen the hybridization efficiency with respect to the standard one-step approach, showing that it is a suitable option for the label-free detection of miRNAs.

One of the main issues concerning real biological samples (i.e. cell extracts or biofluids) consists in the presence of several miRNAs, whose sequence similarity can be very high. The bioassay has therefore to meet strict requirements in terms of selectivity, avoiding non-specific signal due to the binding of different miRNAs. At the same time, interfering sequences can interact with the target, hindering the hybridization with the probe. Such phenomena were studied for the two-step assay, which is the only one that can be directly applied to real samples without long and expensive chemistry related to miRNA labelling. Mixtures of miR-222 and miR-16 were prepared at different concentrations and incubated on the discussed SERS substrates functionalized for the specific detection of miR-222. As shown in Fig. 7, the selective recognition of miR-222 was not affected, under any circumstances, by the presence of miR-16. The intense vibrational features of half2-Cy3 at 1388 cm^{-1} and 1462 cm^{-1} are easily recognizable in the spectrum of samples incubated at 1 µM concentration of miR-222 and no substantial differences are observed by the comparison of their intensity

measured in the absence (curve a) or in the presence of miR-16 (curves b, c). A similar behavior is reported in case of 10 nM miR-222 (red curves), even if a 100 times higher concentration of miR-16 was present in the mixture (curve f). The obtained results suggest that the selectivity of the probe is warranted in a wide range of miR-222 concentrations. These results were confirmed also by the ELISA-like assay performed on mixtures containing different concentrations of miR-222 and miR-16, as reported in the ESI (Fig. S1b).

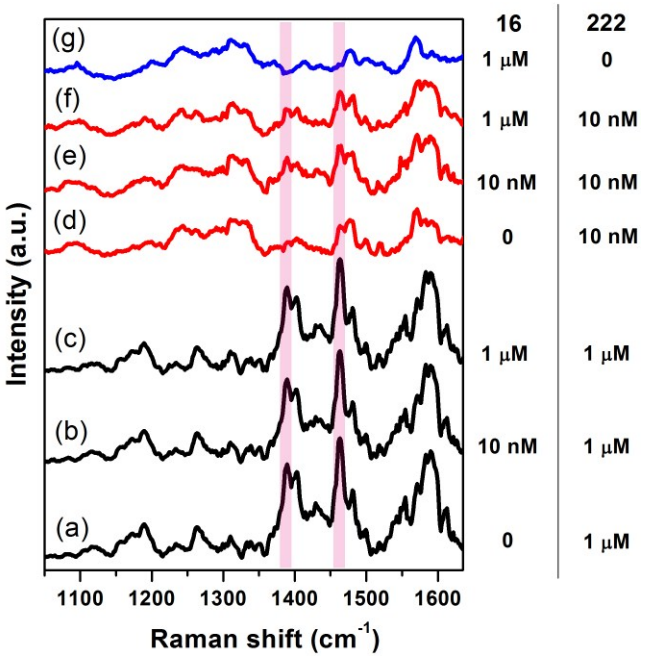

Fig. 7. SERS spectra of the PSD substrates incubated with mixtures of the target miR-222 and an interfering miR-16 at different concentrations. Curves a, d and g represent the reference spectra of samples incubated with 1 μM and 10 nM pure miR-222 alone and 1 μM pure miR-16, respectively. Curves b,c, e and f show the results of the SERS analysis of the mixtures, whose composition is reported on the right side of the graph. The vertical bars highlight the features of half2-Cy3 at 1388 cm^{-1} and 1462 cm^{-1}.

miR-222 detection in cell extracts. Although a good selectivity and sensitivity were demonstrated during the analysis of synthetic oligos in buffer solutions (alone or in mixtures), this is only an approximation of the complexity of real biological matrices. For this reason, before to check the detection of miR-222 in real samples, the synthetic miR-222 was diluted in the total RNA extract of H460 NSCLC cells in a range of concentrations from 250 nM to 0.5 nM. The expression level of miR-222 is very low for such cell line in comparison to other NSCLC cells[27], thus H460 extracts can be considered as a blank sample representative of the interfering matrix effect given by real biological samples. The data obtained in SSC 4x-SDS (Fig. 6b,c) were confirmed within the error bars by the values calculated for the extracts, pointing out that the former calibration curve can be exploited for the quantitation of miR-222 in real samples.

Finally, the two-step procedure was applied to the detection of miR-222 in RNA cell extracts. Total and small RNA enriched extracts of H460 and miR-222 transfected H460 cells were employed. The relative expression of miR-222 in those samples was initially evaluated by RT-qPCR, as reported in Fig. 8a. The samples were diluted 1:2 in SSC 10x, in order to establish the optimized ionic strength needed for the hybridization. The SERS spectra of the samples at the end of the two-step protocol are reported in Fig. 8b, along with a reference spectrum of the half2-Cy3 (black curve). The band at 1462 cm^{-1} is marked by a coloured bar in order to highlight its appearance over the modes of the half1 probe. In particular, the peak can be clearly observed in the spectrum of the total RNA extract of transfected H460 cell, but also as a shoulder of the main peak of the half1 around 1475 cm^{-1} for the small-RNA-enriched sample. In agreement with the very low expression level of miR-222 in the H460 line, no bands attributed to the Raman label could be identified in the spectra of their RNA extracts, nor in the small-enriched sample, neither in the total one, confirming the good specificity of the assay. Moreover, the integrated areas of the 1462 cm^{-1} band of the half2-Cy3 were used to quantify the amount of miR-222 in the cell extracts through the calibration curve presented above. Actually, a concentration of 3.24 nM was calculated for the total extract of H460+miR222 cells, while the conversion of the average area obtained for the small-H460+miR222 cells provided a concentration of 734 pM, that falls however below the LOD. The SERS data are in good accordance with the reference ELISA-like assay (Fig.8c), which shows a higher miR-222 concentration in the total extract (2.78 nM), in comparison with the small-H460+miR222 sample (650 pM).

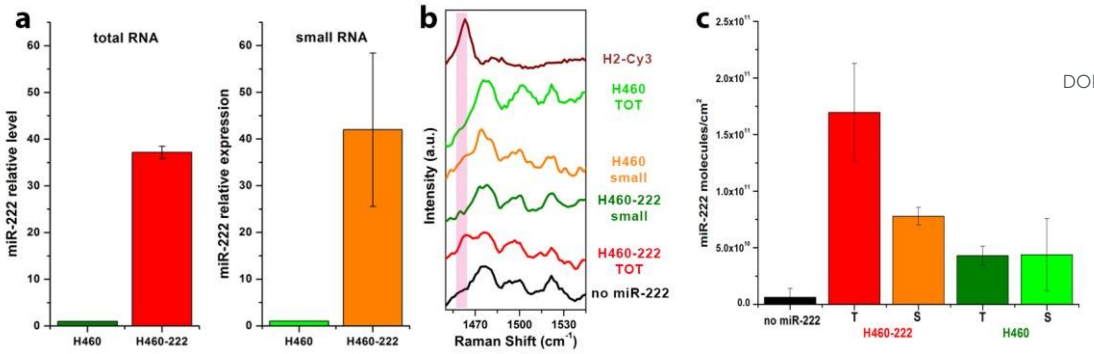

Fig. 8. a) Expression levels of miR-222 in the small and total RNA extracts of H460 evaluated by standard RT-qPCR; b) SERS spectra of small and total RNA extracts of H460 NSCLC cells and miR-222 transfected H460 NSCLC cells (from top to bottom); c) ELISA-like assay performed on the same samples.

Conclusions

Silver decorated porous silicon-PDMS membranes integrated in microfluidic chips were applied to the SERS detection and quantitation of miRNAs. Two bioassays, based on a standard one-step and a new two-step hybridization approach were developed and compared. Contrary to the first assay, the second one allows the introduction of a Raman label in the half2 probe used in the second hybridization, avoiding any chemical modification of the target.

The optimization of the two protocols was assisted by the SERS analysis at each functionalization step, which enabled to identify the optimal probe density by the variation of the salt and probe concentrations in the immobilization buffer, in order to maximize the hybridization events. After that, the sensitivity of the one-step and two-step protocols was investigated.

The best results were obtained with the resonantly excited Cy3 which was used for the analysis of different miR-222 concentrations, obtaining reliable calibration curves. Comparable LODs were calculated for the one- and two-step assays (0.55 and 1.51 nM, respectively), confirming a good hybridization efficiency for the new procedure. The selectivity of the label-free two-step approach was then assessed by the analysis of different mixtures of the target miR-222 with the interfering miR-16.

Finally, total and small RNA extracts of NSCLC H460 cells were analysed in the microfluidic chips, showing the feasibility of detection and quantitation of miRNAs in real biological samples.

Acknowledgements

The research has received funding from the Italian Flagship Project NANOMAX (Progetto Bandiera MIUR PNR 2011–2013) and the Italian FIRB 2011 NEWTON (RBAP11BYNP).

References

1 I. J. Jahn, O. Zukovskaja, X.-S. Zheng, K. Weber, T. W. Bocklitz, D. Cialla-May and J. Popp, *Analyst*, 2017, **142**, 1022–1047.

2 C. Novara, A. Lamberti, A. Chiadò, A. Virga, P. Rivolo, F. Geobaldo and F. Giorgis, *RSC Adv.*, 2016, **6**, 21865–21870.

3 A. Lamberti, A. Virga, A. Chiadò, A. Chiodoni, K. Bejtka, P. Rivolo and F. Giorgis, *J. Mater. Chem. C*, 2015, **3**, 6868–6875.

4 R. M. Jarvis, A. Brooker and R. Goodacre, *Faraday Discuss.*, 2006, **132**, 281–292.

5 E. Martinsson, M. A. Otte, M. M. Shahjamali, B. Sepulveda and D. Aili, *J. Phys. Chem. C*, 2014, **118**, 24680–24687.

6 I. S. Patel, W. R. Premasiri, D. T. Moir and L. D. Ziegler, *J. Raman Spectrosc.*, 2008, **39**, 1660–1672.

7 K. C. Henderson, E. S. Sheppard, O. E. Rivera-betancourt, J. Choi, R. A. Dluhy, K. A. Thurman, M. Winchell and D. C. Krause, *Analyst*, 2014, **139**, 6426–6434.

8 P. Negri and R. A. Dluhy, *Analyst*, 2013, **138**, 1–7.

9 A. Virga, P. Rivolo, E. Descrovi, A. Chiolerio, G. Digregorio, F. Frascella, M. Soster, F. Bussolino, S. Marchiò, F. Geobaldo and F. Giorgis, *J. Raman Spectrosc.*, 2012, **43**, 730–736.

10 L. A. Lane, X. Qian and S. Nie, *Chem. Rev.*, 2015, **115**, 10489–10529.

11 T. Tian, J. Wang and X. Zhou, *Org. Biomol. Chem.*, 2015, **13**, 2226–2238.

12 M. Ha and V. N. Kim, *Nat. Rev. Mol. Cell Biol.*, 2014, **17**.

13 D. P. Bartel, *Cell*, 2004, **116**, 281–97.

14 I. G. Cannell, Y. W. Kong and M. Bushell, *Biochem. Soc. Trans.*, 2008, **36**, 1224–31.

15 J. R. Jackson and N. Standart, *Sci. STKE*, 2007, **re1**, 1–13.

16 H. Dong, J. Lei, L. Ding, Y. Wen, H. Ju and X. Zhang, *Chem. Rev.*, 2013, **113**, 6207–6233.

17 J. Liu, *Curr. Opin. Cell Biol.*, 2008, **20**, 214–221.

18 P. Negri and R. A. Dluhy, *Analyst*, 2013, **138**, 4877–4884.

19 M. Green, F.-M. Liu, L. Cohen, P. Kollensperger and T. Cass, *Faraday Discuss.*, 2006, **132**, 269–280.

20 A. Barhoumi, D. Zhang, F. Tam and N. J. Halas, *J. Am. Chem. Soc.*, 2008, **130**, 5523–5529.

21 S. Catuogno, C. L. Esposito, C. Quintavalle, L. Cerchia, G. Condorelli and V. De Franciscis, *Cancers (Basel).*, 2011, **3**, 1877–1898.

22 L. Bi, Y. Rao, Q. Tao, J. Dong, T. Su, F. Liu and W. Qian, *Biosens. Bioelectron.*, 2013, **43**, 193–199.

23 E. Prado, N. Daugey, S. Plumet, L. Servant and S. Lecomte, *Chem. Commun.*, 2011, **47**, 7425–7427.

24 H.-N. Wang, B. M. Crawford, A. M. Fales, M. L. Bowie, V. L. Seewaldt and T. Vo-dinh, *J. Phys. Chem. C*, 2016, **120**, 21047–21055.

25 X. Li, S. Ye and X. Luo, *Chem. Commun.*, 2016, 10269–10272.

26 A. Chiadò, C. Novara, A. Lamberti, F. Geobaldo, F. Giorgis and P. Rivolo, *Anal. Chem.*, 2016, **88**, 9554–9563.

27 F. Bettazzi, E. Hamid-Asl, C. L. Esposito, C. Quintavalle, N. Formisano, S. Laschi, S. Catuogno, M. Iaboni, G. Marrazza, G. Mascini, G. Cerchia, V. De Franciscis, G. Condorelli and I. Palchetti, *Anal. Bioanal. Chem.*, 2013, **405**, 1025–1034.

28 A. L. Teixeira, J. Silva, M. Ferreira, I. Marques, M. Gomes, J. Mauricio, F. Lobo and R. Medeiros, *Eur. J. Cancer*, 2012, **48**, S216.

29 L. Fabris, Y. Ceder, A. M. Chinnaiyan, G. W. Jenster, K. D. Sorensen, S. Tomlins, T. Visakorpi and G. A. Calin, *Eur. Urol.*, 2016, **70**, 312–322.

30 G. Palmara, A. Chiadò, R. Calmo and C. Ricciardi, 2016, Analytical and Bioanalytical Chemistry. accepted-.

31 A. Chiadò, G. Palmara, S. Ricciardi, F. Frascella, M. Castellino, M. Tortello, C. Ricciardi and P. Rivolo, *Colloids Surfaces B Biointerfaces*, 2016, **143**, 252–259.

32 C. Beleites and V. Sergo, 2016.

33 R. D. C. Team, 2008.

34 H. Sato, M. Kawasaki, K. Kasatani and M. Katsumata, *J. Raman Spectrosc.*, 1988, **19**, 129–132.

35 A. Virga, P. Rivolo, F. Frascella, A. Angelini, E. Descrovi, F. Geobaldo and F. Giorgis, *J. Phys. Chem. C*, 2013, **117**, 20139–20145.

36 A. W. Peterson, R. J. Heaton and R. M. Georgiadis, *Nucleic Acids Res.*, 2001, **29**, 5163–5168.

37 E. Prado, N. Daugey, S. Plumet, L. Servant and S. Lecomte, *Chem. Commun.*, 2011, 1–5.

38 B. Giese and D. McNaughton, *Phys. Chem. Chem. Phys. PCCP*, 2002, **4**, 5171–5182.

39 S. Najjar, D. Talaga, Y. Coffinier, S. Szunerits, R. Boukherroub, L. Servant, V. Rodriguez and S. Bonhommeau, *J. Phys. Chem. C*, 2014, **118**, 1174–1181.

40 H. Grabhorn and A. Otto, *Vacuum*, 1990, **41**, 473–475.

41 C. David, N. Guillot, H. Shen, T. Toury and M. Lamy De La Chapelle, *Nanotechnology*, 2010, **21**, 475501.

42 N. E. Marotta, K. R. Beavers and L. A. Bottomley, *Anal. Chem.*, 2013, **85**, 1440–1446.

43 T. M. Herne and M. J. Tarlov, *J. Am. Chem. Soc.*, 1997, **119**, 8916–8920.

44 D. Y. Petrovykh, H. Kimura-Suda, M. J. Tarlov and L. J. Whitman, *Langmuir*, 2004, **20**, 429–440.

View Article Online
DOI: 10.1039/C7FD00140A